

## COMPUTATIONAL MODELING DETAILS

### 40 CFR 146.84 (c) (1)

#### Project Name: Pineywoods CCS Hub

##### Facility Information

Facility Contact: Pineywoods CCS, LLC  
14302 FNB Parkway  
Omaha, NE 68154

RRC Organization  
Report Number: in process

Entrance Location: 30° 3'45.96"N, 94°33'14.78"W

Well Locations: Liberty and Hardin Counties, Texas

Well Name	Latitude (dms)	Longitude (dms)
PW-1	30° 2'1.24"N	94°31'16.30"W
PW-2	30° 3'45.96"N	94°33'14.78"W
PW-3	30° 6'7.27"N	94°31'27.22"W
PW-4	30° 7'58.94"N	94°31'28.79"W

## Table of Contents

<b>List of Acronyms/Abbreviations.....</b>	<b>4</b>
<b>A. Computational Modeling Details 40 CFR 146.84(c)(1) .....</b>	<b>5</b>
A.1 Static Earth Model.....	5
A.1.a Model Extent.....	7
A.1.b Model Layering.....	8
A.1.b.1 Layer Elevation and Thickness.....	11
A.1.b.2 Grid Cell Size .....	12
A.1.c Model Timeframe .....	13
A.1.d Model Parameterization.....	14
A.2 Modeling Parameters .....	14
A.2.a Porosity .....	14
A.2.b Permeability .....	15
A.2.b.1 Vertical Permeability .....	15
A.2.c Relative Permeability.....	19
A.2.c.1 Frio Sandstone Relative Permeability.....	19
A.2.c.2 Anahuac Confining Unit Layer Relative Permeability .....	19
A.2.d Capillary Pressure Relationships .....	20
A.2.d.1 Storage and Confining Unit's Capillary Pressure.....	20
A.2.e Formation (Pore) Compressibility .....	20
A.2.f Initial Formation (Fluid) Pressure.....	21
A.2.g Formation Initial Temperature.....	21
A.2.h Fracture Pressure and Fracture Gradient.....	22
A.2.i Salinity .....	22
<b>B. References .....</b>	<b>23</b>

## List of Figures

Figure 1: Map of the Static Earth Model and Dynamic Model Boundary.....	6
Figure 2: Injection and In-Zone Well Locations and Reservoir Settings (Vertical Exaggeration 5X).....	6
Figure 3: Map Showing Computational Model Boundary and Faults From GEOMAP (GEOMAP, 2022) ..	7
Figure 4: Geophysical Logs from the Parker Estate 1 Well Used for Geologic Characterization.....	9
Figure 5: Map of 2D Seismic Lines Used to Create SEM .....	10
Figure 6: Pineywoods CCS Hub Stratigraphic Column.....	11
Figure 7: Elevation Map of Upper [Frio] (MSL Depth in ft).....	12
Figure 8: Model Grid View.....	13
Figure 9: Model Permeability-Porosity Transforms in the Frio Formation (Hovorka, 2006). .....	15
Figure 10: Computational Model Porosity (Fraction) by Layer .....	16
Figure 11: Computational Model Permeability (mD) by Layer.....	17
Figure 12: Computational Model Reservoir Pressure Distribution (psi) .....	18
Figure 13: (a) Frio Sandstone (Jung et al, 2017), (b) Anahuac Shale Unit Relative Permeability Curve (Bennion and Bachu, 2005).....	19
Figure 14: Computational Model Frio Formation Capillary Pressure Curve.....	20

## List of Tables

Table 1: Computational Model Domain Data.....	5
Table 2: Pineywoods CCS Hub Computational Model Layering.....	11
Table 3: Top Perforation Depths of Computational Model for Lower Frio .....	12
Table 4 : Average Porosity and Porosity Range for Perforated Frio Interval .....	14
Table 5: Injection Zone Horizontal Permeability Estimates .....	15
Table 6: Frio Formation Initial Reservoir Pressure .....	21
Table 7: Reservoir Initial Temperatures .....	21
Table 8: Injection Pressure Details .....	22
Table 9: Frio Formation Water Salinity.....	22

## List of Acronyms/Abbreviations

2D	Two dimensional
3D	Three dimensional
ac	Acres
AOR	Area of Review
API	American Petroleum Institute
CCS	Carbon Capture and Storage
CO <sub>2</sub>	Carbon dioxide
DOE	Department of Energy
EPA	Environmental Protection Agency
°F	Degrees Fahrenheit
ft	Feet
ft <sup>3</sup>	Cubic feet
ft/yr	Feet per year
GS	Geologic sequestration
in	Inches
lb	Pounds
m	Meter
mi	Mile
mD	Millidarcies
mg/L	Milligrams per liter
MMscf/d	Million standard cubic feet per day
MPa	Megapascals
MSL	Mean sea level
t	Metric tons
t/d	Metric tons per day
MMt	Million metric tons
t/d	Metric tons per day
nD	Nanodarcies
psi	Pounds per square inch, gauge
SEM	Static earth model
UIC	Underground injection control
USDW	Underground source of drinking water

## A. Computational Modeling Details 40 CFR 146.84(c)(1)

This document is prepared in compliance with 40 CFR 146.84(c) to provide an overview of the computational model developed for the Pineywoods CCS Hub in Liberty and Hardin Counties, Texas. Information on the geologic data used to develop the 3D Static Earth Model (SEM) as well as the modeling parameters used to simulate subsurface fluid flow are outlined in this document. Much of this data is included in the **Application Narrative** and *Area of Review and Corrective Action Plan* documents with additional details provided in the discussion below.

The primary software used to develop the computational model was *Petrel*, a geological modeling software suite, and *GEM*, a compositional simulator.

### A.1 Static Earth Model

A 3D model for the proposed Pineywoods CCS Hub was developed to fully contain the footprint of the injected CO<sub>2</sub> and threshold pressure plumes. The model incorporates the details of the subsurface geologic characterization and model parameters outlined below. The aerial extent of the dynamic computational model extracted from the larger SEM, with respect to the proposed injection and observation well locations, is shown by the blue outline on **Figure 1**. The coordinates and model domain information are summarized in **Table 1**.

**Table 1: Computational Model Domain Data**

Coordinate System	WGS_1984_BLM_Zone_14N_ftUS		
Horizontal Datum	World Geodetic System 1984 ensemble		
Coordinate System Units	US FEET		
Coordinate of X min	3001700	Coordinate of X max	3106700
Coordinate of Y min	10909600	Coordinate of Y max	11016100
Elevation bottom of domain	-8,165	Elevation top of domain	-3,359

The model area includes the four proposed injection wells roughly in the southern lower portion of the model, as well as the four in-zone, three above-zone, and six USDW observation wells. In total, data from 51 wells was used to construct the SEM, with well locations shown by the filled red circles in **Figure 1**.

CO<sub>2</sub> injection at the Pineywoods CCS Hub will be into the Lower Frio, a saline reservoir occurring at a depth between approximately 6,000 ft and 7,100 ft SSTVD at the injection site. The Frio Formation is regionally overlain by the Anahuac Formation, which is a significant confining zone as shown in **Figure 2**. The four proposed CO<sub>2</sub> injection wells at the Pineywoods CCS Hub would inject 1.25 MMt/y CO<sub>2</sub> per well for 30 years. The captured CO<sub>2</sub> from multiple sources will be transported by pipeline to the injection site.

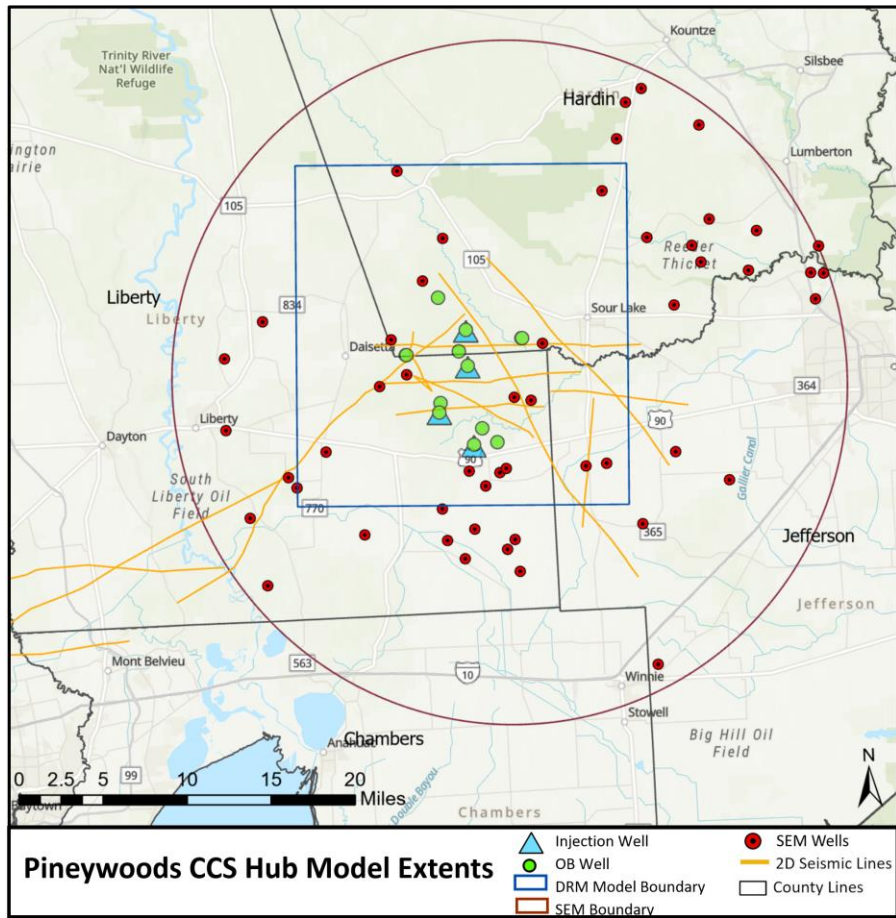


**Figure 1: Map of the Static Earth Model and Dynamic Model Boundary.**

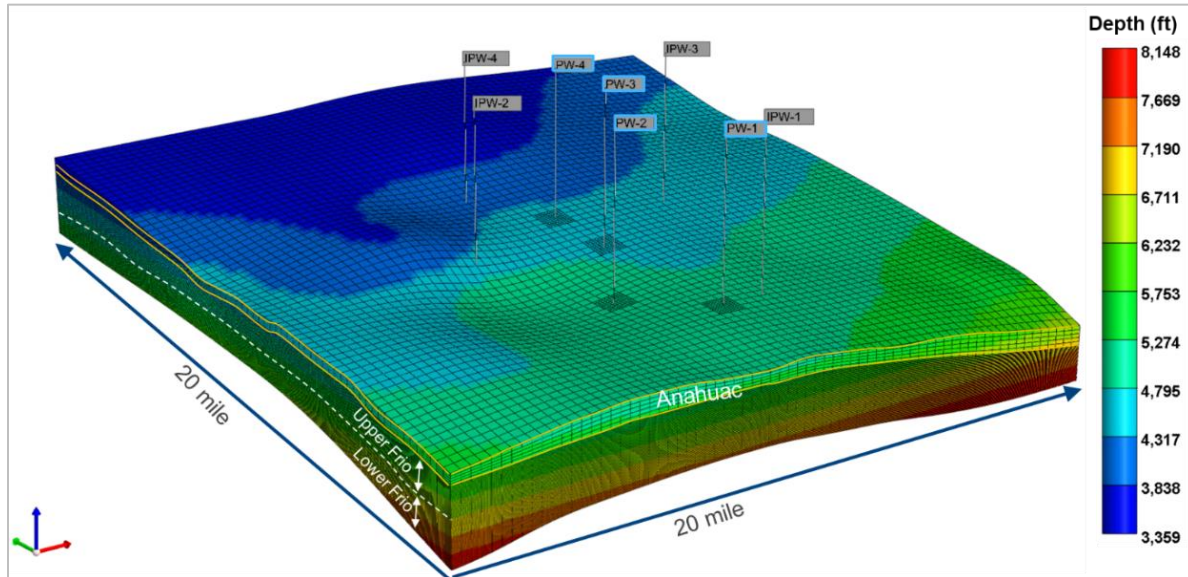


**Figure 2: Injection and In-Zone Well Locations and Reservoir Settings (Vertical Exaggeration 5X)**

### A.1.a Model Extent

The computational model is rectangular in shape with a north-to-south orientation overlaying the Pineywoods CCS Hub. The model extends approximately 20 mi north-to-south and 20 mi east-to-west for a total of 400 mi<sup>2</sup> in **Figure 3**. The model is oriented to account for CO<sub>2</sub> plume migration up dip to the northwest direction and local features created by the salt domes.

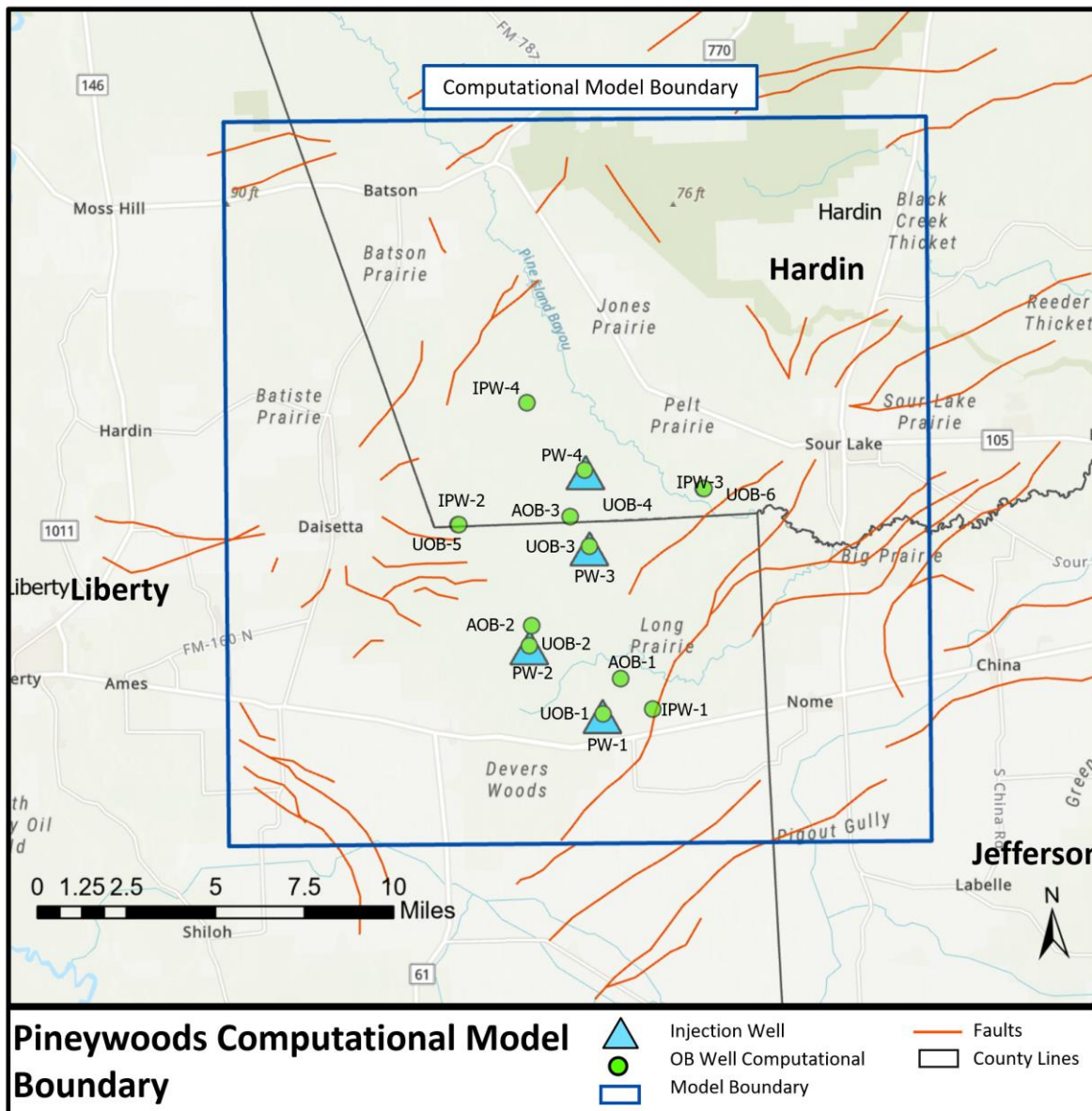


**Figure 3: Map Showing Computational Model Boundary and Faults From GEOMAP (GEOMAP, 2022) .**

The Frio Formation is extensive in the project and surrounding area; thus, open boundaries were assigned to replicate these settings in the computational model. The faults, depending upon the ratio of their throw to the thickness of the permeable formation, may impede the flow. The

sensitivity analysis for fault transmissivity is presented in **Section C.6 of the Post Injection Site Care and Site Closure Plan**. The dynamic reservoir boundary, and faults in the area are shown in **Figure 3**. A pore volume multiplier of 10,000 was applied to the outer layer of vertical grid cells along the perimeter of the model to approximate an open-boundary system behavior. Pore volume modifiers increase the pore volume of the reservoir model without having to include additional grid blocks in the reservoir model. This helps to reduce the grid extent and runtime of the model.

#### ***A.1.b Model Layering***

The proposed injection interval at the Pineywoods CCS Hub will be the Lower Frio Formation only. Information on the injection, confining, and overlying formations at the Pineywoods CCS Hub benefitted greatly from the legacy oil and gas wells in the area. In total, data from 51 wells that partially or completely cover the storage zone are used to construct the SEM. A combination of Gamma ray and SP log data from these 51 wells were used to create a site specific regional cross section, and SP log data were relied upon for the basis of top-of-formation picks. The data collected from these wells, located within a 20-mile radius from the injection wells, comprise the SEM area. The Dynamic Reservoir Model (DRM), or computational model, is a subset of the SEM. The SEM is representative of the reservoir properties within the Pineywoods CCS Hub and includes a full suite of geophysical well logs, including gamma ray, bulk density, dipole sonic, and porosity. One sample representative log used for the SEM is shown in **Figure 4**.

Density porosity, neutron porosity, gamma ray, and Spontaneous Potential (SP) logs were used to populate the 3D porosity model. SP log was used to first define the facies because the log had more coverage of the storage formation and primary seal. The analog core data from the Frio Pilot Test, situated approximately 20 miles in the southwest direction formed the basis correlating the effective porosity and permeability (Hovorka, 2009). Due to the vicinity of the Frio Pilot Test, mineralogical data analog data was also used.

In addition to the well log and analog Frio Pilot Test data, Tenaska licensed more than 350 mi of existing 2D seismic lines that transect the Pineywoods CCS Hub. This data was used to interpret site-specific and regional geologic structure, determine lateral continuity, and build the geologic inputs used for computational modeling. The seismic data included 10 lines: oriented along the strike and slip of the regional dip as shown in **Figure 5**.

These 2D seismic lines provided data to refine the structural interpretation of the Pineywoods CCS Hub. Additionally, seismic data was used to confirm the lateral continuity of the injection and confining zones. The 2D seismic lines were tied to sonic measurements taken in the ARCO FFE1 (**Figure 7 in the Application Narrative**). The structural interpretation of the Pineywoods CCS Hub was combined with the porosity and permeability model developed using the well log data and analog core data. Together, these data sets were used to build a 3D SEM in *Petrel* representative of the geologic and petrophysical characteristics within the Pineywoods CCS Hub.

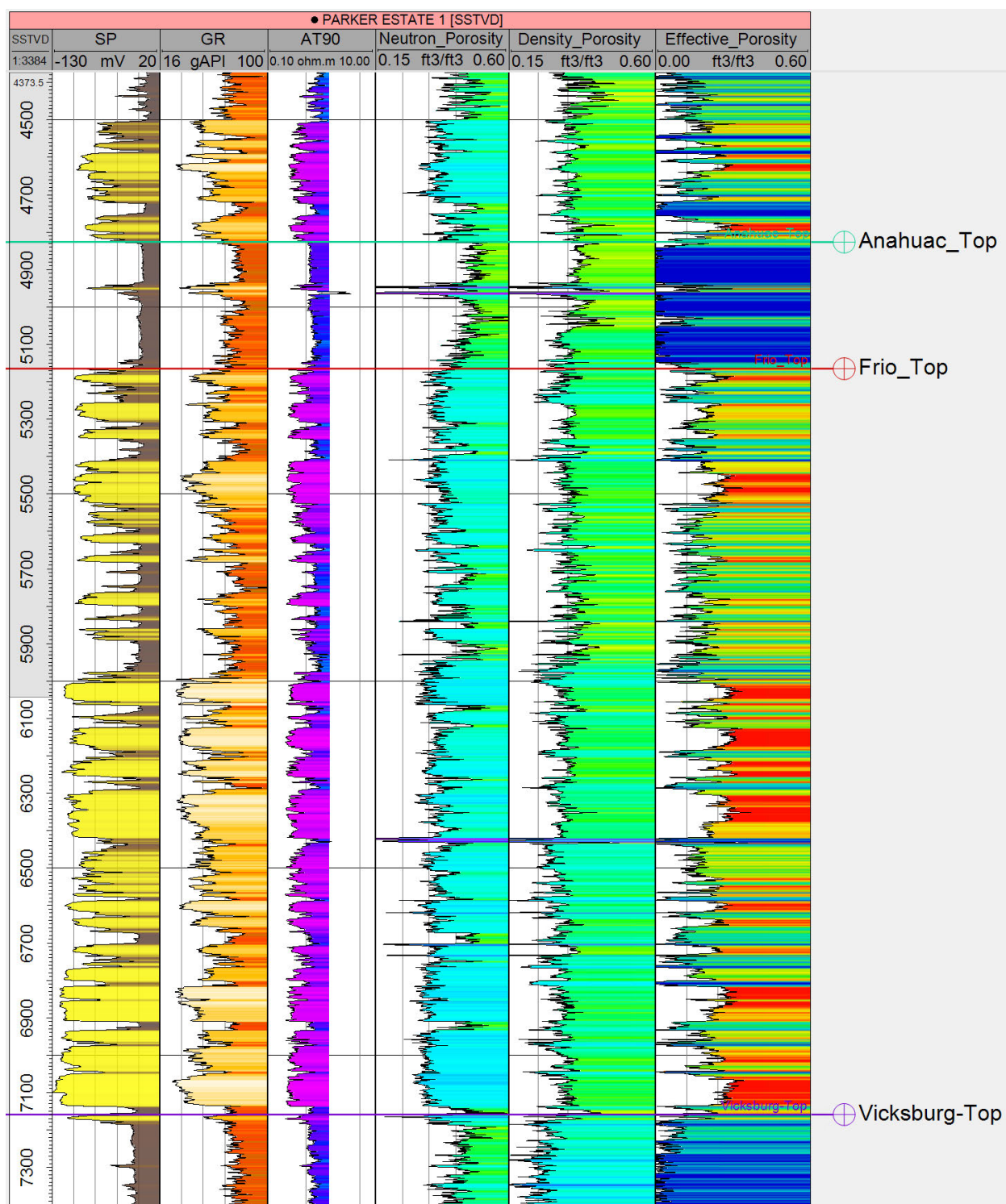
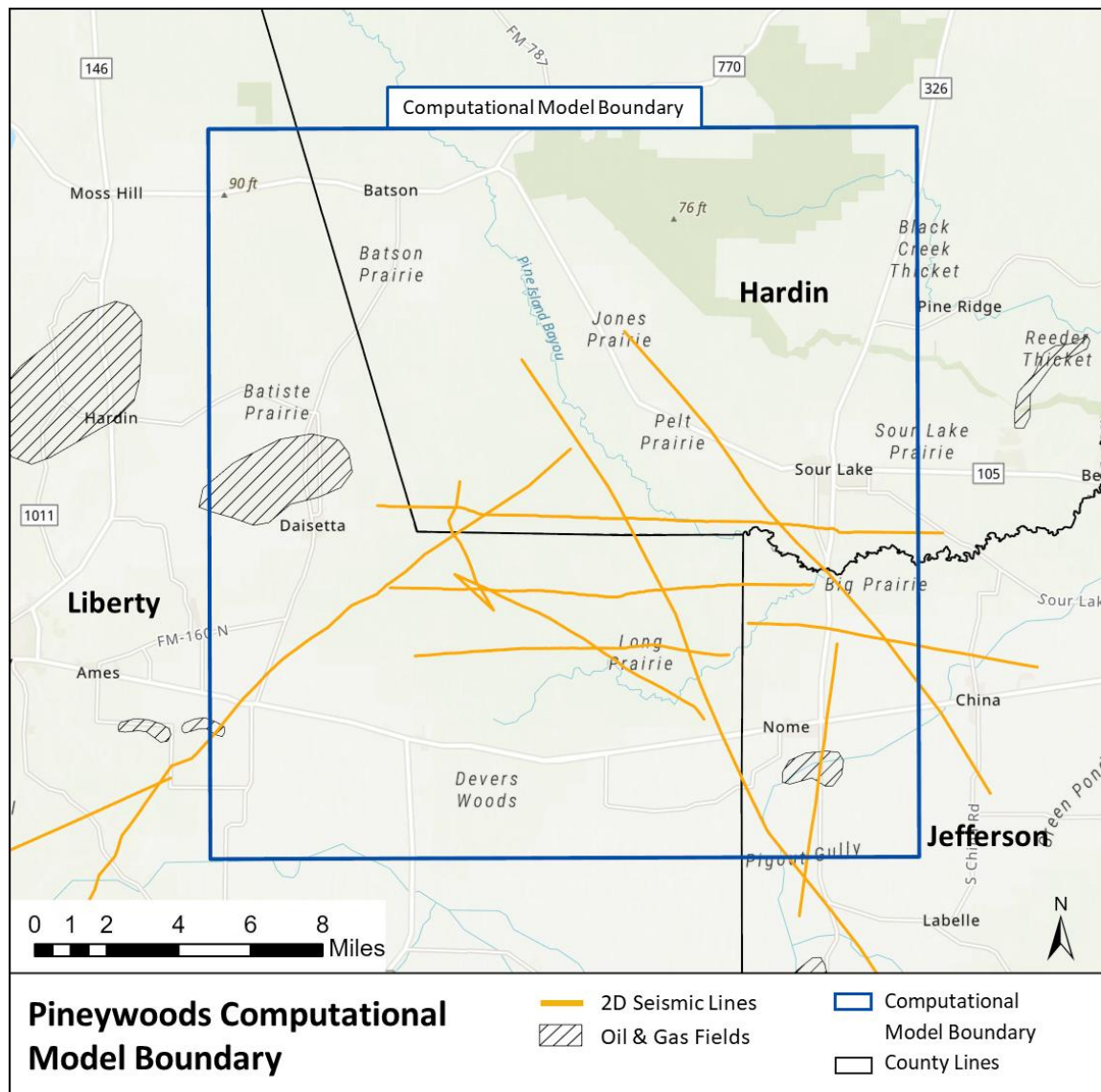


Figure 4: Geophysical Logs from the Parker Estate 1 Well Used for Geologic Characterization



**Figure 5: Map of 2D Seismic Lines Used to Create SEM**

The primary CO<sub>2</sub> injection interval for the Pineywoods CCS Hub is the Lower Frio as shown in **Figure 6**. The Frio Formation has favorable reservoir properties, such as a several hundred-foot package of porous sands, giving it high storage resource potential and sufficient permeability to support high rates of CO<sub>2</sub> injectivity per well below 90% of the fracture pressure.

The Frio Formation is overlain by a nearly 400 ft thick transgressive Anahuac shale that serves as a confining unit for the Frio. A high capillary entry pressure of 3,500 psi was reported for the Anahuac Formation in the nearby Frio-Pilot Test project (Hovorka, 2009), demonstrating it to be a good quality seal. Moreover, the Anahuac Formation is regulatorily defined as confining for many Class I UIC wells and serves as seal for many oil and gas reservoirs (Hovorka, 2009). There are regionally present marine shales in the Miocene strata shallower than the primary caprock that may act as secondary and tertiary seals.

System	Series	Stratigraphic Unit	Aquifers, Reservoirs and Confining Zones	Depths (SSTVD)
Tertiary	Miocene	Undifferentiated	Chicot Freshwater Aquifer	
		Upper Miocene	Evangeline Freshwater Aquifer	Lowermost USDW Base at ~2,100'
		Middle Miocene	Minor Saline Reservoir	
		Amphistegina B	Confining Unit	
		Lower Miocene 2	Minor Saline Reservoir	
		Marginuline A	Confining Unit	
		Lower Miocene 1	Minor Saline Reservoir	
	Oligocene	Anahuac Formation (shale)	Primary Upper Confining Unit	Top at 4,810'
		Upper Frio Formation (interbedded shales)	Minor Saline Reservoir	Top at 5,200'
		Lower Frio Formation (mostly sands)	Primary Saline Reservoir: Proposed Injection Zone	Top at 6,000' Base at 7,100'
		Vicksburg Formation	Primary Lower Confining Unit	

Figure 6: Pineywoods CCS Hub Stratigraphic Column

The computational model includes a total of 70 vertical layers that covers the primary seal, Upper Frio and Lower Frio shown in Table 2.

Table 2: Pineywoods CCS Hub Computational Model Layering

Flow Unit	Layer Number	Formation	Type
Anahuac	0-5	Anahuac	Confining Unit
Upper Frio	6-31	Upper Frio	Future Injection Interval
Lower Frio	32-70	Lower Frio	Injection Interval

#### A.1.b.1 Layer Elevation and Thickness

The elevation map for the storage unit is generated using *Petrel* software. Figure 7 shows the top elevation map of the Upper Frio sandstone. The top of the perforation in the Lower Frio Formation

and storage zone thickness for all injection wells are summarized in **Table 3**. A side view of the 3D computational model imported into the reservoir simulator GEM is shown in **Figure 2**.

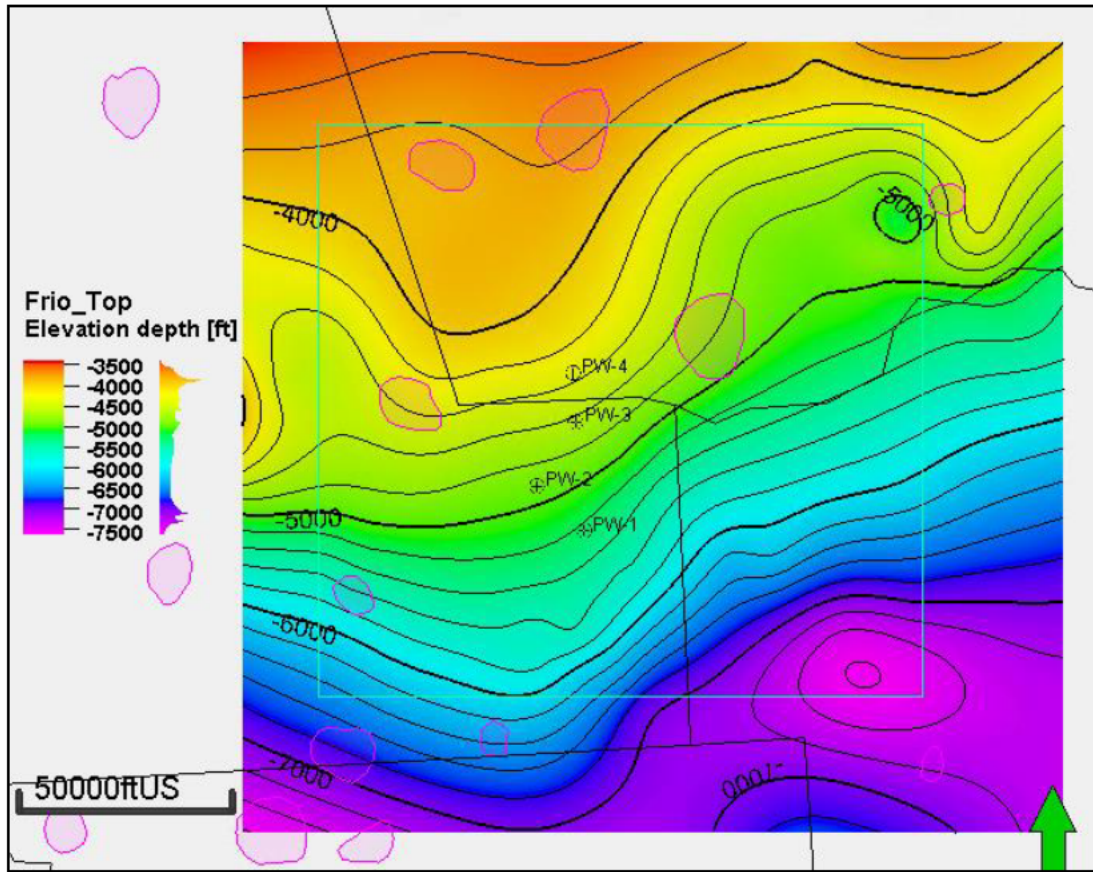


**Figure 7: Elevation Map of Upper [Frio] (MSL Depth in ft)**

**Table 3: Top Perforation Depths of Computational Model for Lower Frio**

Operating Information	PW-1	PW-2	PW-3	PW-4
Perforated interval Top (ft MSL)	6,032	5,879	5,580	5,338
Interval Thickness (ft)	1,048	788	872	845

#### *A.1.b.2 Grid Cell Size*

Grid cell size is an important element of reservoir model setup. Literature survey sheds light on the impact of gridding on the plume movement (Doughty et al, 2007; Juanes et al, 2006; Doughty and Pruess, 2004; Yamamoto and Doughty, 2009). Their findings suggest that some grid refinement is required around the injection well to better simulate buoyancy and near well-bore effects, while coarser grids can be implemented further away, closer to the model boundaries. To minimize computational processing time and to better define the CO<sub>2</sub> movement, individual grid blocks in x and y-direction were approximately 1,500 ft long, and the thickness of each grid layer in the injection zone was approximately 15 ft in **Figure 8**.

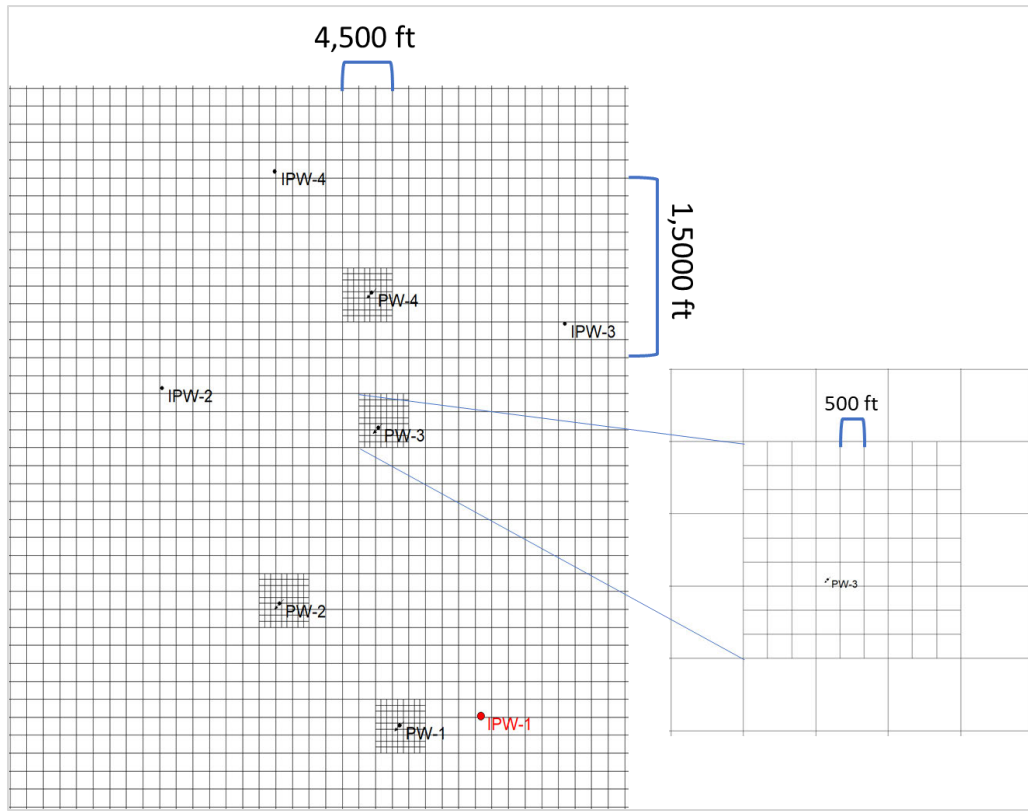


**Figure 8: Model Grid View**

Within the caprock, thickness of each layer was approximately 200 ft, shown in **Figure 2**. Local grid refinement for each injection well was used in such a manner that well block sizes were 500 ft in each of X and Y-direction in the vicinity of the injection wells and up to 1,500 ft through all layers of the simulation model, as shown in **Figure 8**. With 70 vertical layers, 70 grid cells in the X-direction, and 71 grid cells in the Y-direction, the overall model grid had a total of 347,900 grid blocks. The model dimensions were 20 miles north-south and 20 miles east-west providing a modeling area of nearly 400 square miles (256,000 acres).

#### **A.1.c Model Timeframe**

Per 40 CFR 146.84(c)(1), the computational model simulation is required to run from the beginning of injection activities until the plume movement ceases, pressure differentials sufficient to cause the movement of injected fluids or formation fluids into a USDW are no longer present, or until the end of a fixed time period as determined by the UIC Program Director. Research by Flett *et al.* (2007) has shown that it may be necessary for the model simulation to run for a significant time period following the end of CO<sub>2</sub> injection to determine if the CO<sub>2</sub> plume is migrating in a predictable manner given the reservoir structure and other geologic factors (Flett; Freeze). The model was run for 30 years of CO<sub>2</sub> injection plus 50 years of PISC (see **Section B.3 of the Post-Injection Site Care and Site Closure Plan**). The model was run for an additional 30 years beyond the proposed 20-year PISC timeframe to provide visualization of the CO<sub>2</sub> plume movement predictability and reduced rate of migration compared to the active injection period.

#### **A.1.d Model Parameterization**

The final construction step consisted of populating the computational model with all the site-specific parameters defined in **Section A.2** below (including porosity, permeability, and reservoir pressure, among others). **Figure 10**, **Figure 11**, and **Figure 12** show the implementation of the computational model porosity, permeability, and initial reservoir pressure. The model figures include a 5Xvertical exaggeration to show layer details.

A discussion of the methodology and rationale used to determine various reservoir parameters within the computational model is provided in **Section A.2** below.

### **A.2 Modeling Parameters**

Relevant hydrogeologic model parameters for multiphase flow modeling include porosity, permeability, relative permeability, capillary pressure, formation compressibility, formation brine salinity, formation (fluid) pressure, and formation temperature (EPA 2013). A detailed description of the relevant parameters selected for the initial assessment, the source of this information, and the rationale for their use are provided below. This section is directly linked to the **Area of Review and Corrective Action Plan** as it details all the inputs from the computational model which was built and used to define the AOR at the Pineywoods CCS Hub.

#### **A.2.a Porosity**

Porosity values in the Frio were derived from an average of the neutron porosity and density porosity logs. One of the logs used is shown above in **Figure 4**. Density porosity, neutron porosity, gamma ray, and Spontaneous Potential (SP) logs were used to populate the 3D porosity model. SP log was used to first define the facies because the log had more coverage of the storage formation and primary seal. The overlap of the density and neutron porosity logs indicates clean sand, and it was set as a reference for clean sand identification (Bassiouni, 1994). Similarly, a shale baseline porosity was defined based on the density porosity log for a pure shale interval within the storage zone. Next, shale volume ( $V_{shale}$ ) values were calculated from the shale content in the zone. Then, effective porosity for intermediate facies were determined using the  $V_{shale}$  formulation that accounts for the shale content in the strata. (**Equation 1**). Then, effective porosity for intermediate facies was determined using the  $V_{shale}$  formulation that accounts for the shale content in the strata.

$$\phi_{effective} = \phi_{Total} - V_{Shale} \times \phi_{Shale} \quad (\text{Equation 1})$$

The average effective porosity values and range of porosity values are summarized in **Table 4** for the Lower Frio. A cross sectional view of the effective porosity distribution is shown in **Figure 10**.

**Table 4 : Average Porosity and Porosity Range for Perforated Frio Interval**

Injection Interval	Average Porosity (%)	Porosity Range (%)
Lower Frio	0.202	0.001 – 0.35

#### A.2.b Permeability

A permeability-porosity correlation for the Frio Formation based on the Frio Pilot Test core data was used (Hovorka, 2006). The porosity-permeability relationship is shown in **Table 5**. These transform functions were used to calculate the average horizontal permeability within the reservoir.

**Table 5: Injection Zone Horizontal Permeability Estimates**

Injection Interval	Average Horizontal Permeability (mD)	Horizontal Permeability Range (mD)
Lower Frio	219	0.001 - 2330

A vertical to horizontal permeability ratio of 0.2 was then used to calculate the vertical permeability from the horizontal permeability. Horizontal permeability values are summarized in **Table 6** for the Frio Formation.

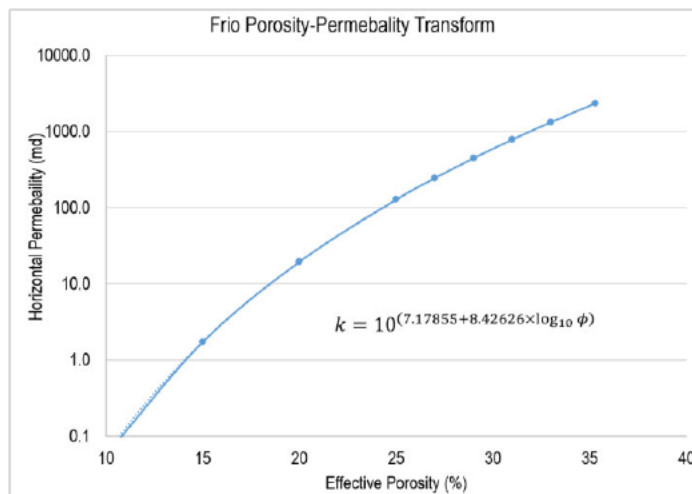


**Figure 9: Model Permeability-Porosity Transforms in the Frio Formation (Hovorka, 2006).**

#### A.2.b.1 Vertical Permeability

Vertical permeability at the Pineywoods CCS Hub is currently unknown. To account for the nature of deltaic depositional setting, a vertical permeability anisotropy ( $k_v/k_h$ ) value of 0.2 was used to compute the vertical permeability from the horizontal permeability in the computational model. A sensitivity analysis was performed to account for the impact of uncertainty associated with this value. The results of sensitivity analysis are reported in **Section C.4 of PISC and Site Closure Plan**. This value will be confirmed during the core analysis performed when the test well is drilled, prior to CO<sub>2</sub> injection, as outlined in the **Pre-Operational Testing Plan**.

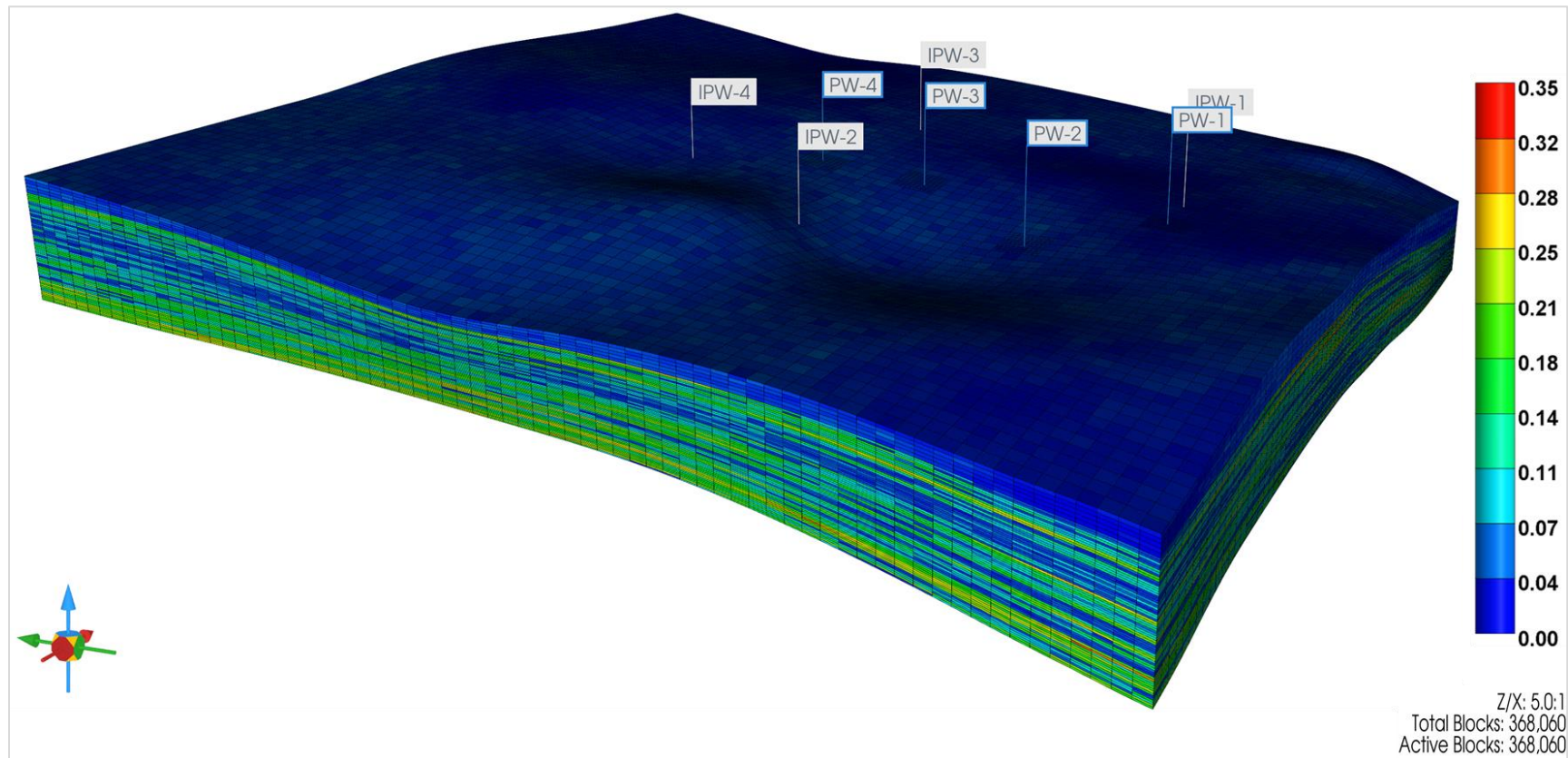


**Figure 10: Computational Model Porosity (Fraction) by Layer**

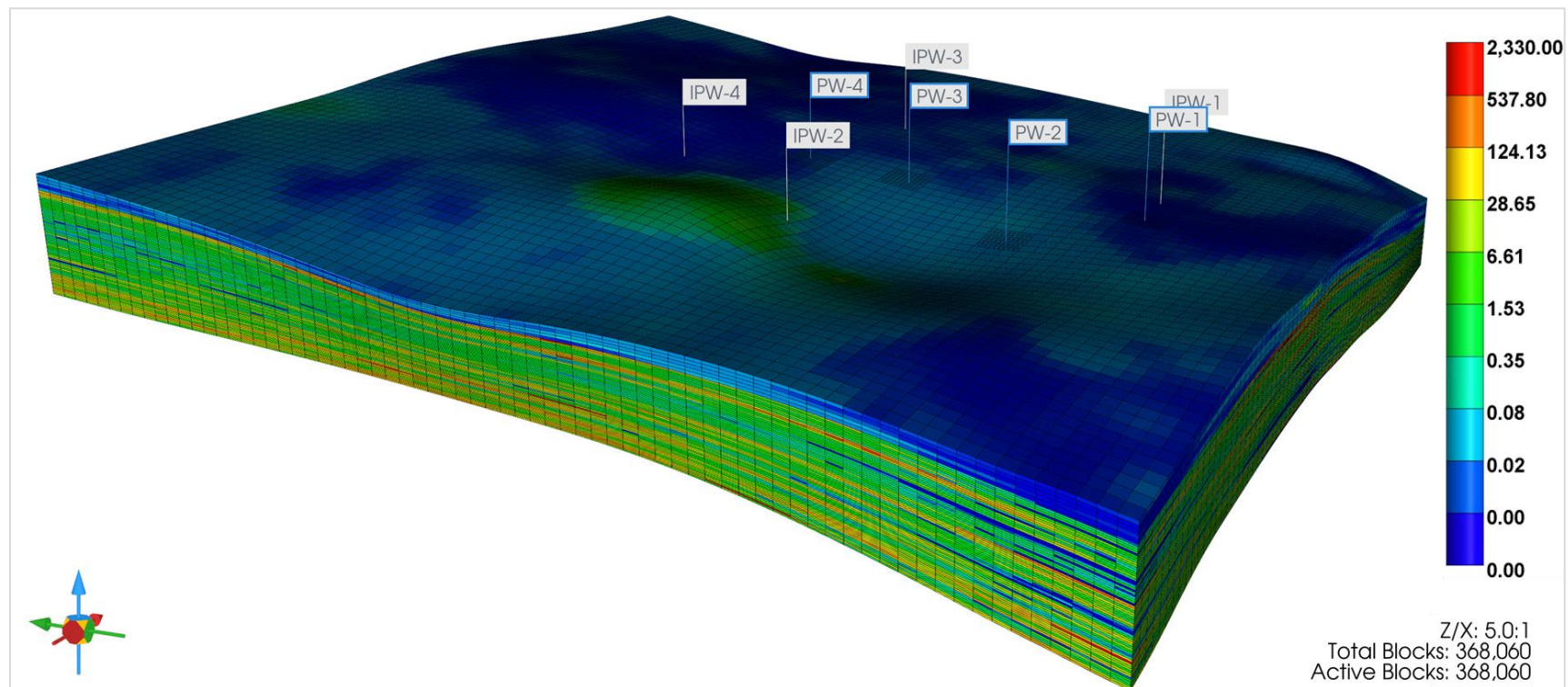


**Figure 11: Computational Model Permeability (mD) by Layer**

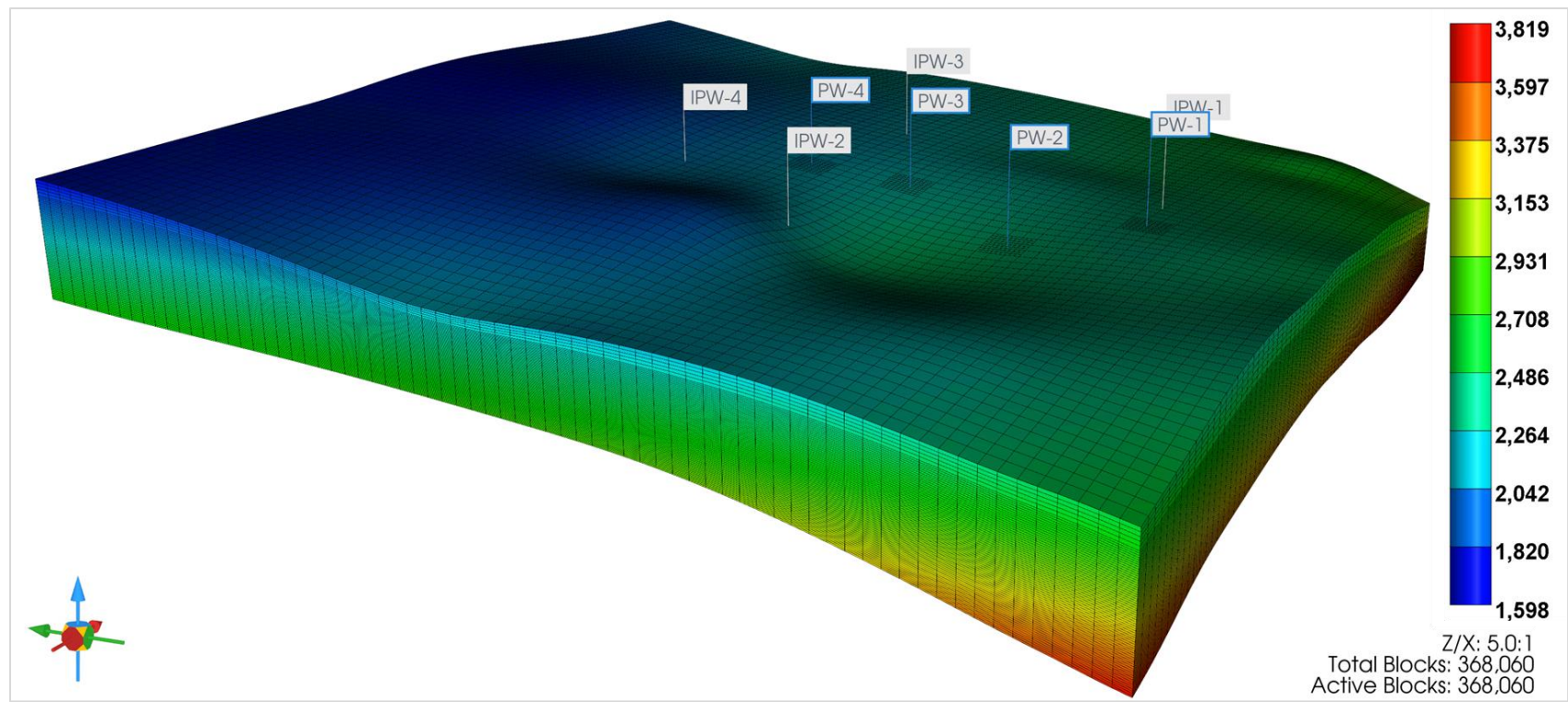


**Figure 12: Computational Model Reservoir Pressure Distribution (psi)**

### A.2.c *Relative Permeability*

#### A.2.c.1 *Frio Sandstone Relative Permeability*

The relative permeability data used for this study were based on Frio Pilot Test (Jung et al, 2017) core data, which is approximately 20 miles southwest of PW-1 and has similar petrophysical properties and depths. The resulting curves are shown in **Figure 13(a)**.

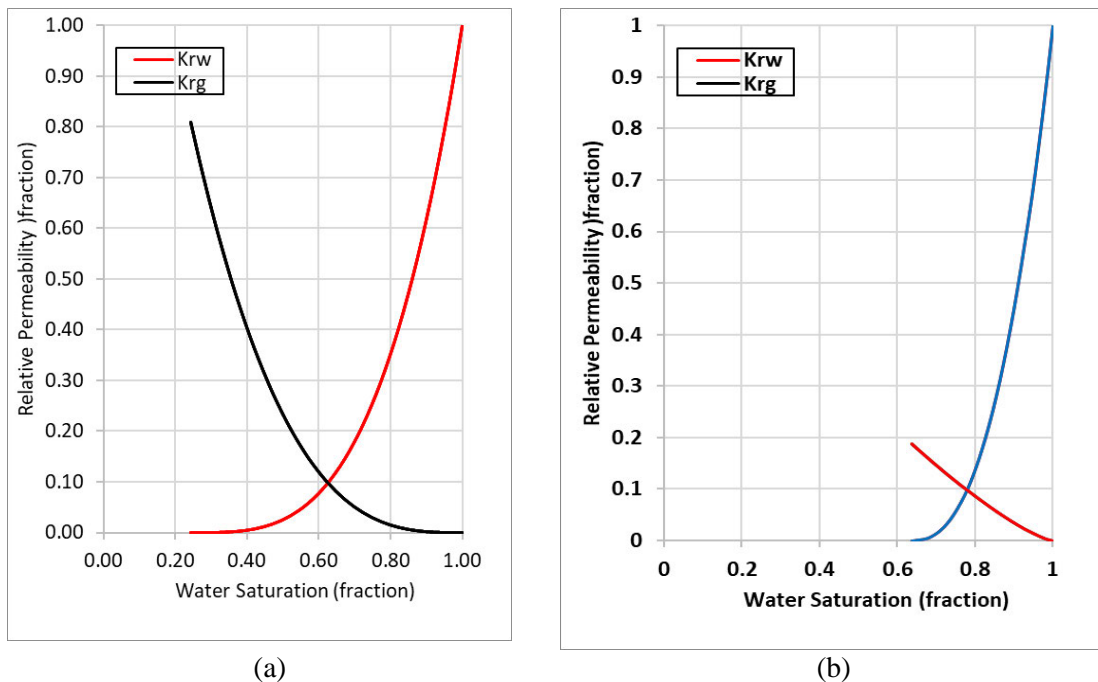


**Figure 13: (a) Frio Sandstone (Jung et al, 2017), (b) Anahuac Shale Unit Relative Permeability Curve (Bennion and Bachu, 2005)**

#### A.2.c.2 *Anahuac Confining Unit Layer Relative Permeability*

Relative permeability data was not available for the confining units at the Pineywoods CCS Hub. The relative permeability curves for a representative shale rock were used (Bennion and Bachu, 2005). This set of curves represents a very low permeability shale rock with high irreducible water saturation and very low gas relative to permeability. Relative permeability curves for the confining unit are illustrated in **Figure 13 (b)**. Due to the high capillary entry pressure reported for the Anahuac (Hovorka, 2009), it is expected that its relative permeability will be more resistive than the curve used. The Anahuac relative permeability curves will be confirmed during the core analysis performed when the test well is drilled, prior to CO<sub>2</sub> injection, as outlined in the **Pre-Operational Testing Plan**.

It is suggested in literature (Krevor et al. 2012) that some of the lower values for the gas relative permeability curve may be an artifact of lab equipment limitations. Therefore, it is suggested that in the reservoir simulations a higher value of K<sub>rg</sub> than reported in literature can be used. A

sensitivity analysis of the CO<sub>2</sub> relative permeability endpoint was performed, and results are reported in **Section C.4 of the PISC and Site Closure Plan**.

#### **A.2.d Capillary Pressure Relationships**

##### **A.2.d.1 Storage and Confining Unit's Capillary Pressure**

The capillary pressure data for the Frio Formation was adopted from the Frio Pilot Test data (Jung et al, 2017) and is shown in **Figure 14**. It is reported in literature that the Anahuac Formation has a very high capillary entry pressure of 3,500 psi (Hovorka, 2009). These high entry capillary pressures mean that the CO<sub>2</sub> pressure in the injection zone needs to exceed these values to enter the 100% brine saturated caprock pores. As a conservative approach, capillary pressures are excluded for the shale layers to allow CO<sub>2</sub> migration into the caprock with small pressure increases. However, because of the very low permeability of the shale layers in the Upper Frio, CO<sub>2</sub> stays within the Frio Formation and well below the confining unit.

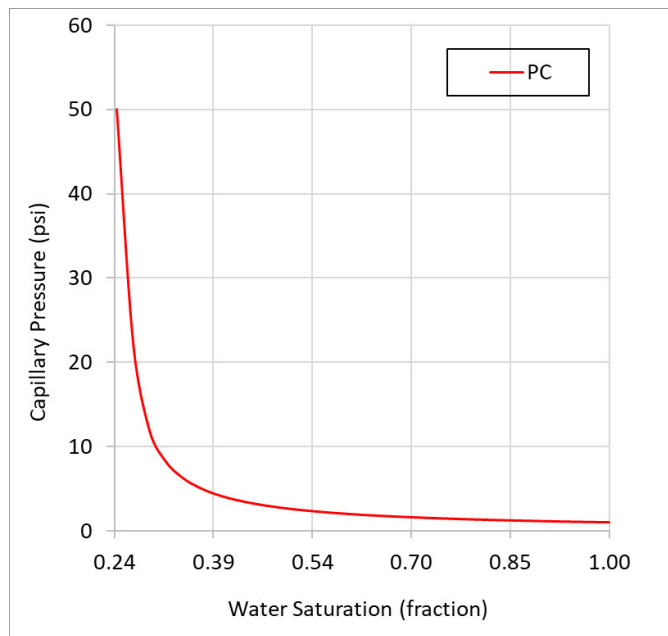


**Figure 14: Computational Model Frio Formation Capillary Pressure Curve**

#### **A.2.e Formation (Pore) Compressibility**

Formation compressibility is a measure of change in rock volume with a change in fluid pressure. Injection-zone formations are subjected to constant external (lithostatic) pressure and internal fluid pressure within the pore spaces. When the internal fluid pressure is reduced (e.g., through oil or gas production), the bulk volume of the rock decreases while the relative volume of the solid rock material (e.g., sand grain or sandstone) increases, effectively reducing the porosity. Rock compressibility data for an injection zone are generally obtained from laboratory measurements on core samples, or where unavailable, estimated from porosity and overburden pressure (EAP, 2013).

Pore compressibility data for the Frio Formation was estimated using the Hall (1953) correlation (**Equation 2**).

$$\text{Equation 2} \quad c_f = (1.782/\phi^{0.438})10^{-6} \quad (2)$$

The correlation is based on laboratory data and is considered reasonable for normally pressured sandstones. With total porosity in the Frio Formation varying from 20% to 35%, the corresponding compressibility varies between 3.606E-6/psi and 2.82E-5/psi. The weighted average of 3.163E-6/psi was used in the model. This value will be confirmed during the core analysis performed when the test well is drilled, prior to CO<sub>2</sub> injection, as outlined in the **Pre-Operational Testing Plan**.

#### *A.2.f Initial Formation (Fluid) Pressure*

The pressure gradient of the Frio Formation at the Pineywoods CCS Hub is 0.465 psi/ft based on regional trends data for the normally pressured formations in the Gulf of Mexico (Burke et al., 2012). A similar trend is observed in a nearby well (API-4219932965) from a very thin gas reservoir in the top of the Frio Formation (TRC, 2023). This pressure gradient was used for initial pressure conditions in the reservoir model as shown in **Table 6**.

**Table 6: Frio Formation Initial Reservoir Pressure**

Hydrogeologic Unit	Reference Depth (ft)	Pressure Gradient (psia/ft)	Formation Pressure (psia)	Source
Frio (Upper & Lower)	6,186	0.46745	2,892	Burke et al., 2012
Frio (Upper)	4,764	0.46730	2,226	Initial production potential test of well with API # 4219932965

#### *A.2.g Formation Initial Temperature*

The formation initial temperature is estimated from the well log header data of several legacy oil and gas wells in the area (API #: 4219932031, 4219932859, 4219992859, 4219932508, 4219932965, 4219925422). This data is summarized in **Table 7**. Reservoir reference depths and temperature values based on the 1.3275 °F/100ft temperature gradient was used as inputs in the reservoir model. Reservoir temperature values were then automatically calculated for the reservoir layers in the model by depth.

**Table 7: Reservoir Initial Temperatures**

Hydrogeologic Unit	Reference Depth (ft)	Temperature (°F)	Temperature Gradient (°F/100ft)
Frio	6186	152.12	1.3275

#### ***A.2.h Fracture Pressure and Fracture Gradient***

Fracture pressure is estimated based on the data reported for a nearby well with API number 29132765 (TRC, 2023) as well as regional value. A value of 0.7 psi/ft was used, although higher values are also reported in literature (Jung, 2017). Therefore, a sustained pressure gradient of 0.63 psi/ft (90% of the 0.7) is expected to not result in any observed geomechanical formation impacts. More information on the plans to calculate fracture pressure can be found in **Section F of the Pre-Operational Testing Plan**. To ensure that fracture pressure is not surpassed during the injection of CO<sub>2</sub>, a conservative bottomhole pressure limit equal to 90% of the assumed fracture pressure gradient of 0.7 psi/ft was imposed. For the reservoir simulation, the wells were operated using this constraint, with an additional injection rate constraint of 1.25 Mt/y. The pressure constraints used in simulations are shown in **Table 8**.

**Table 8: Injection Pressure Details**

Injection Pressure Details	PW-1	PW-2	PW-3	PW-4
Fracture gradient (psi/ft)	0.7	0.7	0.7	0.7
Maximum injection pressure (90% of fracture pressure) (psi)	3,847	3,750	3,562	3,410
Elevation corresponding to maximum injection pressure (ft MSL)	6,106	5,953	5,654	5,412
Elevation at the top of the perforated interval (ft MSL)	6,106	5,953	5,654	5,412
Calculated maximum injection pressure at the top of the perforated interval (psi)	4,274	4,167	3,958	3,788

#### ***A.2.i Salinity***

USGS' produced water database for the Frio Formation was used, and as a conservative approach, the maximum value reported in a nearby well (API# 420710197), located approximately 14 miles southeast of PW-1, was directly input to the model. This sampling data provided a salinity value of approximately 113,781 mg/L for the Frio Formation at a depth of approximately 8,210 ft (**Table 9**).

**Table 9: Frio Formation Water Salinity**

Formation	TDS (mg/l)	Source
Frio	113,781	USGS National Produced Waters Geochemical Database for Well with API# 420710197 (Blondes et al. 2019))

## B. References

Doughty, C., & Pruess, K. 2004. Modeling supercritical carbon dioxide injection in heterogeneous porous media. *Vadose Zone Journal*, 3(3):837–847.

Doughty, C., Freifeld, B.M., & Trautz, R.C. 2007. Site characterization for CO<sub>2</sub> geologic storage and vice versa – the Frio brine pilot, Texas, USA as a case study. *Environmental Geology*, DOI 10.10007/s00254-007-0942-0.

EPA (U.S. Environmental Protection Agency). 2013. Geologic Sequestration of Carbon Dioxide, Draft Underground Injection Control (UIC) Program Class VI Well Area of Review Evaluation and Corrective Action Guidance for Owners and Operators. EPA 816-R-13-005, Washington, D.C.

Flett M., Gurton, R., & Weir, G. 2007. Heterogeneous saline formations for carbon dioxide disposal: Impact of varying heterogeneity on containment and trapping. *Journal of Petroleum Science and Engineering*, 57:106-118.

Freeze, R.A., and Cherry, J.A., 1979, *Groundwater*: Englewood Cliffs, NJ, Prentice-Hall, 604 p.

GEOMAP, 2022. Generalized Structural Contours of the Subsurface, Executive Maps.

Hall, Howard N., 1953. Compressibility of Reservoir Rocks. *J Pet Technol* 5 (1953): 17–19. doi: <https://doi.org/10.2118/953309-G>

Hovorka, Susan D., 2009. Optimal Geological Environments for Carbon Dioxide Disposal in Saline Aquifers in the United States, Final Technical Progress Report. Bureau of Economic Geology, Jackson School of Geosciences, The University of Texas at Austin.

Juanes, R., Spiteri, E.J., Orr Jr., F.M., & Blunt, M.J. 2006. Impact of relative permeability hysteresis on geological CO<sub>2</sub> storage. *Water Resources Research*, 42. W12418.

Yamamoto, H., & Doughty, C. 2009. Investigation of gridding effects for numerical simulation of carbon dioxide geologic sequestration,” Proceedings of TOUGH Symposium, LBNL., September 2009, Berkeley, CA.